ACS Macro Letters

Letter

pubs.acs.org/macroletters

Tunable pH-Responsive Polymeric Micelle for Cancer Treatment

Xiaolan Zhang,[†,‡,§,∥] Yixian Huang,[†,‡,§,∥] Mohammed Ghazwani,[†,‡,§] Peng Zhang,[†,‡,§] Jiang Li,[†,‡,§] Stephen H. Thorne,[§] and Song Li*[,†,‡,§]

[†]Center for Pharmacogenetics, [‡]Department of Pharmaceutical Sciences, School of Pharmacy, and [§]University of Pittsburgh Cancer Institute, University of Pittsburgh, Pittsburgh, Pennsylvania 15261, United States

Supporting Information

ABSTRACT: The development of bioresponsive polymers is important in drug delivery systems. Herein, we reported the construction of a series of pH-sensitive micelles by conjugating the hydrophilic polyethylene glycol (PEG) segment to a hydrophobic farnesylthiosalicylate derivative, FTS-hydrazide (FTS-H), with a hydrazone linker, whose cleavability can be conveniently modulated by choosing various lengths of the carbon chain or appropriate electron-withdrawing groups with different steric environment around the hydrazone linker. We examined the hydrolysis rates of these pH-sensitive micelles in both neutral and acidic conditions. One of the pH-sensitive micelles (PHF-2) was found to be highly sensitive to acidic conditions while being fairly stable in neutral conditions. Furthermore, PHF-2 micelles well retained the antitumor activity of free FTS-H. We further evaluated the use of PHF-2 micelles as a carrier for delivering paclitaxel (PTX) and the triggered release of PTX under the acidic environment. PTX-loaded PHF-2 micelles showed enhanced antitumor activity compared with free PTX, likely because of the combinational effect between PHF-2 micelles and loaded PTX.

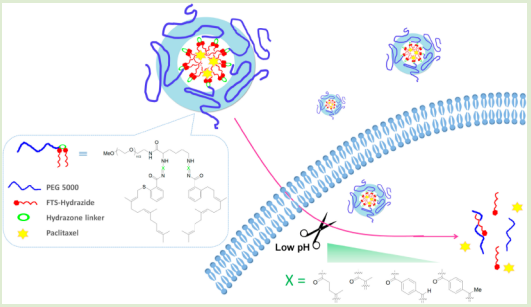

Drug delivery using micelles with a nanoscopic supramolecular core−shell structure has gained increasing attention due to their simplicity, small sizes (10−100 nm), and the ability to improve the pharmacokinetics and efficacy of anticancer drugs.[1,2] In general, polymeric micelles are composed of a hydrophobic core capped with a hydrophilic shell such as polyethylene glycol (PEG). Water-insoluble drugs can be loaded into the core of micelles via hydrophobic−hydrophobic interaction, and the hydrophilic shell grafted onto the surface prolongs the stability of the micelles in blood. Selective release of drugs in response to a specific stimulus is an attractive and effective way to exert their high therapeutic efficiency and minimize unwanted side effects.[3,4] The strategy of using a cleavable linker between drug and polymer has been favorably employed to achieve this purpose.[5−7] A hydrazone linkage is an excellent candidate due to its acid-sensitive nature.[8,9] It is expected to be stable in the blood but instantly cleaved at an acidic tumor microenvironment or the endosome/lysosome compartment. Furthermore, the approach involved in the covalent conjugation of drug to polymer through hydrazone linkage is simple and convenient. Currently, most frequently reported drug delivery systems using a hydrazone linker are concentrated on doxorubicin (DOX) conjugated polymers.[9−11] This is due to the fact that the ketone group of DOX can be readily used to form a hydrazone linker. However, due to the fixed structure of DOX, there is no facile way to achieve tunable DOX release based on the chemistry method.

We have previously shown that PEG-derivatized FTS was a promising drug delivery platform.[12−16] FTS is a hydrophobic compound with Ras antagonist activity.[17−19] It can suppress the growth of many tumor types via inhibiting Ras-dependent signaling involved in tumor development and progression.[20,21] Thus, different from most reported drug delivery systems that lack therapeutic effect, PEG5k-FTS2 micelles themselves exhibited antitumor activity, which means they may collaborate with the loaded drug to achieve a combinational effect.[12,14] Recently, we have shown that incorporation of an additional reduction sensitive (disulfide) linkage into PEG5k-FTS2 led to an increase in tumor cell growth inhibitory effect and a further improvement in its performance in delivery of PTX to tumor cells *in vitro* and *in vivo*,[16] which suggests that the cleavability of the linkage between PEG and FTS affects the overall antitumor activity. In this communication, we reported a different strategy to develop an improved dual functional carrier by introducing a hydrazone linker as a pH-responsive functionality, which can be triggered to release drug under an acidic tumor environment.

We started this study by first identifying FTS derivatives with improved anticancer activity.[22−25] It has been reported that FTS amide, an FTS derivative with an amide added to the carboxyl group, exhibited enhanced cell-growth inhibitory effects without loss of selectivity toward the active Ras.[24] Thus, we kept the structure of FTS amide and designed four FTS amide derivatives (Figure S1, Supporting Information). Among these FTS amide derivatives, FTS-H is the most potent one (Figure 1 and unpublished data). The MTT assay showed

Received: March 6, 2015
Accepted: May 15, 2015
Published: May 18, 2015

ACS Publications © 2015 American Chemical Society

DOI: 10.1021/acsmacrolett.5b00165
ACS Macro Lett. 2015, 4, 620−623

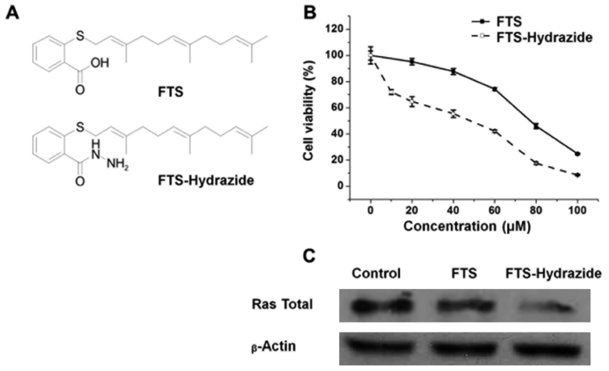

Figure 1. Chemical structure of FTS and FTS-hydrazide (A). Inhibition of PC-3 cell growth by FTS and FTS-hydrazide (B). Effect of FTS and FTS-hydrazide on total Ras expression in PC-3 cells examined by Western blot (C).

that FTS-H was a more effective growth inhibitor of PC-3 cells as compared to FTS (Figure 1B). Furthermore, FTS-H showed an increased downregulation of Ras protein expression levels in PC-3 as compared to FTS (Figure 1C). Thus, FTS-H was chosen to build pH-sensitive micelles. We utilized a straightforward strategy for construction of pH-sensitive micelles by directly conjugating the hydrophilic PEG segment to a hydrophobic FTS-H with a cleavable hydrazone linker. The major advantage of this system lies in the fact that the pH sensitivity of the hydrazone linker can be conveniently controlled by modulating the different chemical environment around the hydrazone linker. We designed and synthesized PHF-1 and PHF-2 conjugates that differed in the carbon chain length around the hydrazone linker. In addition, two electron-withdrawing groups (benzene ketone or aldehyde) with different steric environment around the hydrazone linker were introduced to build PHF-3 and PHF-4 conjugates, respectively. Then we compared the hydrolysis rates of the hydrazone bond in different PHFs in both neutral and acidic conditions. Furthermore, we evaluated the use of tunable PHF micelles as a carrier for delivering paclitaxel (PTX) and triggered release of PTX under the acidic environment.

Synthesis of PHF 1−4 conjugates (Figure 2) is straightforward, using the ketone group on PEGylated molecules to react

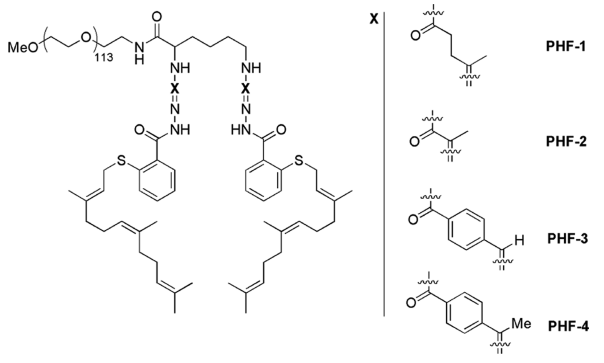

Figure 2. Structures of pH-sensitive PHF conjugates.

with FTS-H, which was usually completed within 2 h. ^{1}H NMR spectra of PHF conjugates are shown in Figures S2−5 (Supporting Information), with signals at 1.4−2.2 ppm, 3.6 ppm, and 7.2−8.5 ppm attributable to the methylene protons of PEG, carbon chain, and benzene ring protons of FTS-H, respectively. The absorbance of amino groups in the FTS-H was shown at 3312 cm^{-1} (Figure S7, Supporting Information). Once FTS-H was coupled to the PEG backbone, the peak of the amino group disappeared, which implies the successful conjugation between PEG and FTS-H (Figures S8−11, Supporting Information). Furthermore, the molecular weights of PHF conjugates and PEG were determined by MALDI-TOF (Figures S12−16, Supporting Information), which further indicates the successful synthesis of PHF conjugates.

The acid sensitivity of PHF conjugates was examined by HPLC. FTS-H has a UV absorbance. Once FTS-H was cleaved from the PHF conjugates, the absorbance of the remaining PHF conjugates decreased, which provides a method to evaluate the degradation of these pH-sensitive PHF micelles in both neutral and acidic conditions. As shown in Figure 3A−

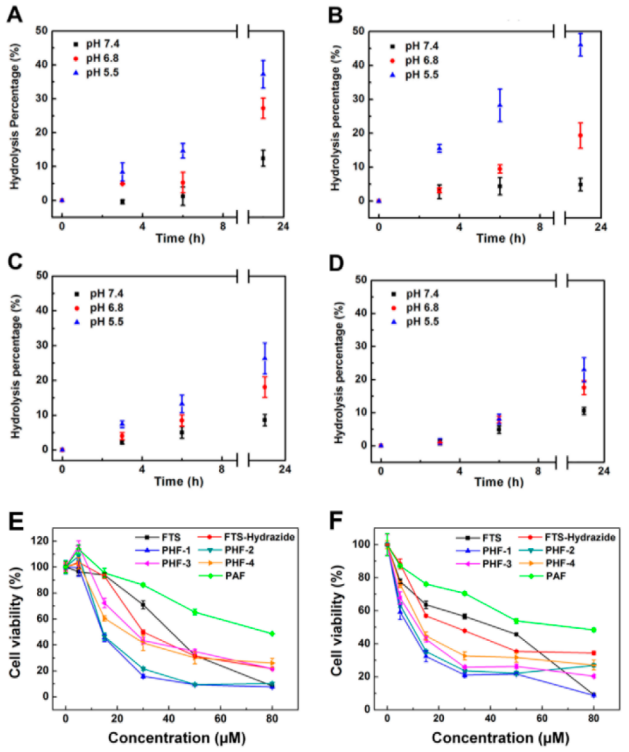

Figure 3. Time- and pH-dependent degradation of PHF-1 (A), PHF-2 (B), PHF-3 (C), and PHF-4 (D) conjugates. Cytotoxicity of free FTS, FTS-hydrazide, and different conjugates in 4T1.2 (E) and PC-3 cells (F).

D, the degradation of all PHF micelles was faster at lower pH. At pH 7.4, only ∼10% of PHF micelles were degraded after 22 h of incubation. In contrast, 25−50% of PHF micelles were degraded at pH 5.5. These results indicate that PHF micelles with hydrazone linker may remain stable in blood but gradually become cleaved at an acidic tumor microenvironment. Among these PHF micelles with a hydrazone linker, PHF-2 showed the most prominent degradation of 46% at pH 5.5 and the least degradation of 6% at pH 7.4 at 22 h (Figure 3B). Increasing carbon chain length around the hydrazone linkage (i.e., PHF-1) led to suppression of the degradation at pH 5.5 relative to PHF-2 (Figure 3A). This is likely because the incorporation of the hydrophobic carbon chain will make the micelle cores more stable and thus suppress acid-sensitive hydrolysis. Substituting the carbon chain with a benzene ring group (i.e., PHF-3 or 4) close to the hydrazone linker further decreased the acid

DOI: 10.1021/acsmacrolett.5b00165
ACS Macro Lett. 2015, 4, 620−623

sensitivity (Figure 3C and D). This may be attributable to the fact that conjugation of the π bonds of the −C═N− bond of the hydrazone with the π-bonding benzene ring decreased the susceptibility of the hydrazone linker to attack, thus suppressing the acid-sensitive degradation.

The antitumor activities of PHF and non-pH-sensitive PAF micelles were tested in both 4T1.2 and PC-3 cancer cell lines and compared to free FTS and FTS-H (Figure 3E and F). Free FTS-H inhibited the tumor cell growth in a concentration-dependent manner. pH-sensitive PHF conjugates resulted in a significant improvement in cytotoxicity. The PAF conjugate with a stable amide linkage was significantly less active compared to both free FTS-H and PHF conjugates. Furthermore, PHF conjugates without a benzene ring showed a more prominent cell inhibition effect compared to those with benzene ring structure. This may be attributed to that FTS-H is much more readily released from pH-sensitive conjugates following intracellular delivery, which is consistent with a pH-dependent degradation study (Figure 3A−D). The IC50 of free FTS, FTS-hydrazide, and different conjugates are summarized in the Supporting Information Table S1. On the basis of the degradation and cytotoxicity studies, PHF-2 was selected for subsequent studies on its potential as a dual functional carrier.

The critical micelle concentration (CMC) is a good indicator for micelle stability. The CMC of the PHF-2 conjugate was determined to be 0.2 μM using pyrene as a fluorescence probe. The small CMC value of the PHF-2 conjugate will ensure the stability of the micelle even upon dilution by a large amount of blood (Figure S17, Supporting Information). The size and size distribution were determined by dynamic light scattering (DLS) (Figure S18, Supporting Information). These PHF-2 micelles possessed very small size of ∼20 nm, which would be beneficial for effective penetration through neovasculatures to reach tumor cells. The efficiency of PHF-2 micelles in drug loading was examined using PTX as a model drug. PTX could be easily loaded into the PHF-2 micelles with a carrier/drug molar ratio as low as 1:1 (Table 1). PTX-loaded PHF-2 micelles were more stable with the increase in the carrier/drug molar ratio. The size and size distribution were not affected when PTX was loaded into the PHF-2 micelles (Table 1). TEM showed spherical structure for these PTX- loaded PHF-2 micelles (Figure 4A). The size observed by TEM shows good agreement with that measured by DLS.

Table 1. Physicochemical Characterization of Drug-Free and PTX-Loaded PHF-2 Micelle

micelle	molar ratio	size (nm)	PDI	DLE (%)	DLC (%)	stability (h)
PHF-2		20.8	0.14			
PHF-2/PTX	1:1	22.0	0.18	82.8	10.3	0.5
PHF-2/PTX	2.5:1	21.5	0.10	85.3	4.8	6
PHF-2/PTX	5:1	21.9	0.13	96.4	2.7	20
PHF-2/PTX	10:1	21.2	0.13	97.8	1.4	72

The profile of PTX release from PTX-loaded PHF-2 micelles was investigated at different pH. As shown in Figure 4B, the release rate of PTX from PHF-2 micelles was pH- and time-dependent. At pH 7.4, 68% of PTX was still in the micelles after 22 h of incubation. However, the PTX release rate was much higher at pH 5.5. The percentage of PTX remaining in the micelles was around 41% and 20% after 6 and 22 h of incubation, respectively, indicating that the PTX-loaded PHF-2 micelles were able to retain most PTX in neutral condition and become triggered to release PTX under the acidic environment. The faster release of PTX from PHF-2 micelles at lower pH is due to facilitated acid-sensitive degradation of the PHF-2 micelles. *In vitro* cytotoxicity of PTX-formulated PHF-2 micelles was investigated on PC-3 and 4T1.2 cancer cell lines and compared to free PTX (Figure 4C, Figure S19, Supporting Information). The IC50 of free PTX and PTX-formulated PHF-2 micelles are summarized in the Supporting Information Table S2. PTX-formulated PHF-2 micelles were more active than free PTX. This might be attributed to the benefit of released FTS-H following the inclusion of pH-sensitive hydrazone linkage. PHF-2 not only acted as a carrier to deliver anticancer drugs but also well retained the biological activity, which could synergize with the loaded drug to achieve better antitumor activity.

In summary, a series of pH-sensitive PHF conjugates have been synthesized and characterized. Their pH sensitivity can be conveniently modulated by changing the carbon chain length or choosing the appropriate electron-withdrawing groups with different steric environment around the hydrazone linker. Among these pH-sensitive PHF conjugates, PHF-2 with high sensitivity to acidic condition and reasonable stability in neutral pH was chosen to deliver PTX. We demonstrated the acid-triggered release of PTX from PHF-2 delivery systems. Additionally, PTX-formulated PHF-2 micelles showed an enhanced cell inhibition effect compared with free PTX. PHF-2 may represent a promising pH-responsive drug delivery system that warrants further study.

■ ASSOCIATED CONTENT

Supporting Information

Additional figures including ^{1}H NMR, MALDI-TOF, IR, DLS, TEM, CMC, and MTT. The Supporting Information is

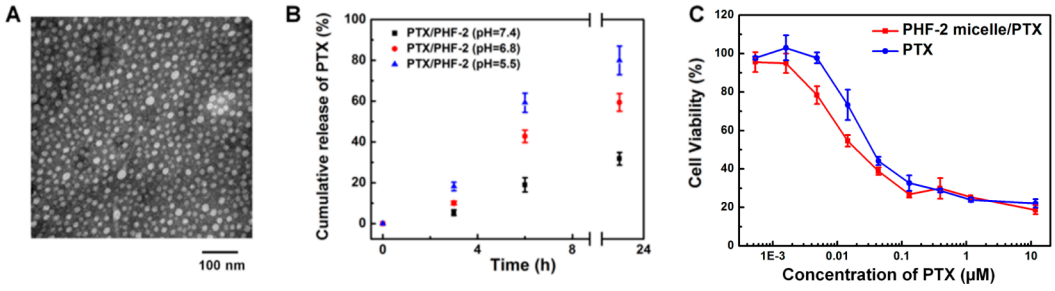

Figure 4. (A) TEM image of PTX-loaded PHF-2 micelles. (B) Release of PTX from PTX-loaded PHF-2 micelles at different pH values. (C) Cytotoxicity of PTX-loaded PHF-2 micelles compared with free PTX in PC-3 prostate cancer cell line.

DOI: 10.1021/acsmacrolett.5b00165
ACS Macro Lett. 2015, 4, 620−623

available free of charge on the ACS Publications website at DOI: 10.1021/acsmacrolett.5b00165.

AUTHOR INFORMATION

Corresponding Author

*Tel.: 412-383-7976. Fax: 412-648-1664. E-mail: sol4@pitt.edu.

Author Contributions

[‖]These authors contributed equally. The manuscript was written through contributions of all authors. All authors have given approval to the final version of the manuscript.

Notes

The authors declare no competing financial interest.

ACKNOWLEDGMENTS

This work was supported by NIH grants RO1CA173887, RO1GM102989, and R21CA173887.

We would like to thank Drs. Donna Stolz and Ming Sun for their help with negative EM study. We would like to thank Ke Liu for establishment of a HPLC method. This project used the UPCI Cancer Biomarkers Facility that is supported in part by award P30CA047904.

REFERENCES

(1) Cabral, H.; Matsumoto, Y.; Mizuno, K.; Chen, Q.; Murakami, M.; Kimura, M.; Terada, Y.; Kano, M. R.; Miyazono, K.; Uesaka, M.; Nishiyama, N.; Kataoka, K. *Nat. Nanotechnol.* **2011**, *6*, 815−23.

(2) Torchilin, V. P. *Pharm. Res.* **2007**, *24*, 1−16.

(3) Bae, Y.; Fukushima, S.; Harada, A.; Kataoka, K. *Angew. Chem., Int. Ed. Engl.* **2003**, *42*, 4640−3.

(4) Sankaranarayanan, J.; Mahmoud, E. A.; Kim, G.; Morachis, J. M.; Almutairi, A. *ACS Nano* **2010**, *4*, 5930−6.

(5) Chen, J.; Zhao, M.; Feng, F.; Sizovs, A.; Wang, J. *J. Am. Chem. Soc.* **2013**, *135*, 10938−41.

(6) Aguirre-Chagala, Y. E.; Santos, J. L.; Huang, Y. X.; Herrera-Alonso, M. *ACS Macro Lett.* **2014**, *3*, 1249−1253.

(7) Wei, H.; Zhuo, R. X.; Zhang, X. Z. *Prog. Polym. Sci.* **2013**, *38*, 503−535.

(8) Howard, M. D.; Ponta, A.; Eckman, A.; Jay, M.; Bae, Y. *Pharm. Res.* **2011**, *28*, 2435−46.

(9) Du, J. Z.; Du, X. J.; Mao, C. Q.; Wang, J. *J. Am. Chem. Soc.* **2011**, *133*, 17560−3.

(10) Bae, Y.; Nishiyama, N.; Fukushima, S.; Koyama, H.; Yasuhiro, M.; Kataoka, K. *Bioconjugate Chem.* **2005**, *16*, 122−30.

(11) Li, S. Y.; Liu, L. H.; Jia, H. Z.; Qiu, W. X.; Rong, L.; Cheng, H.; Zhang, X. Z. *Chem. Commun.* **2014**, *50*, 11852−11855.

(12) Zhang, X.; Lu, J.; Huang, Y.; Zhao, W.; Chen, Y.; Li, J.; Gao, X.; Venkataramanan, R.; Sun, M.; Stolz, D. B.; Zhang, L.; Li, S. *Bioconjugate Chem.* **2013**, *24*, 464−72.

(13) Zhang, X.; Huang, Y.; Zhao, W.; Chen, Y.; Zhang, P.; Li, J.; Venkataramanan, R.; Li, S. *Mol. Pharmaceutics* **2014**, *11*, 2807−14.

(14) Chen, Y.; Zhang, X.; Lu, J.; Huang, Y.; Li, J.; Li, S. *AAPS J.* **2014**, *16*, 600−8.

(15) Zhang, X.; Huang, Y.; Zhao, W.; Liu, H.; Marquez, R.; Lu, J.; Zhang, P.; Zhang, Y.; Li, J.; Gao, X.; Venkataramanan, R.; Xu, L.; Li, S. *Biomacromolecules* **2014**, *15*, 4326−35.

(16) Zhang, X.; Liu, K.; Huang, Y.; Xu, J.; Li, J.; Ma, X.; Li, S. *Bioconjugate Chem.* **2014**, *25*, 1689−96.

(17) Marom, M.; Haklai, R.; Ben-Baruch, G.; Marciano, D.; Egozi, Y.; Kloog, Y. *J. Biol. Chem.* **1995**, *270*, 22263−70.

(18) Haklai, R.; Weisz, M. G.; Elad, G.; Paz, A.; Marciano, D.; Egozi, Y.; Ben-Baruch, G.; Kloog, Y. *Biochemistry* **1998**, *37*, 1306−14.

(19) Marciano, D.; Benbaruch, G.; Marom, M.; Egozi, Y.; Haklai, R.; Kloog, Y. *J. Med. Chem.* **1995**, *38*, 1267−1272.

(20) Blum, R.; Kloog, Y. *Drug Resist. Updates* **2005**, *8*, 369−80.

(21) Gana-Weisz, M.; Halaschek-Wiener, J.; Jansen, B.; Elad, G.; Haklai, R.; Kloog, Y. *Clin. Cancer Res.* **2002**, *8*, 555−65.

(22) Mackenzie, G. G.; Bartels, L. E.; Xie, G.; Papayannis, I.; Alston, N.; Vrankova, K.; Ouyang, N.; Rigas, B. *Neoplasia* **2013**, *15*, 1184−95.

(23) Mor, A.; Aizman, E.; Chapman, J.; Kloog, Y. *Curr. Med. Chem.* **2013**, *20*, 1218−24.

(24) Goldberg, L.; Haklai, R.; Bauer, V.; Heiss, A.; Kloog, Y. *J. Med. Chem.* **2009**, *52*, 197−205.

(25) Ling, Y.; Wang, Z.; Zhu, H.; Wang, X.; Zhang, W.; Wang, X.; Chen, L.; Huang, Z.; Zhang, Y. *Bioorg. Med. Chem.* **2014**, *22*, 374−80.

DOI: 10.1021/acsmacrolett.5b00165
ACS Macro Lett. 2015, 4, 620−623